The Evolution of PAHs and SN-Condensed Dust in Galaxies

Eli Dwek[1] & Frédéric Galliano[2]

ABSTRACT

Spectral and photometric observations of nearby galaxies show a correlation between the strength of their mid-IR aromatic features, attributed to PAH molecules, and their metal abundance, leading to a deficiency of these features in low-metallicity galaxies. We suggest that the observed correlation represents a trend of PAH abundance with galactic age, reflecting the delayed injection of carbon dust into the ISM by AGB stars in the final post-AGB phase of their evolution. We also show that larger dust particles giving rise to the far-IR emission follow a distinct evolutionary trend closely related to the prompt injection of dust by massive stars into the ISM.

Subject headings: ISM: dust – infrared: galaxies – galaxies: starburst – galaxies: evolution – stars: post-AGB – supernovae remnants

1. Introduction

Observing evolutionary processes in galaxies can take longer than even the lifetime of a graduate student. Fortunately, nearby galaxies exhibit a wide range of metallicities and global properties, such as their spectral energy distribution (SED) and their stellar and interstellar medium (ISM) masses. Considering metallicity as an indicator of galactic age, these galaxies can be considered as snapshots of their evolution at different epochs.

An exciting result provided by *ISO* spectral observations of nearby galaxies was the discovery of a striking correlation between the strength of their mid-IR aromatic features

[1]Observational Cosmology Lab., Code 665, NASA Goddard Space Flight Center, Greenbelt MD 20771. e-mail: eli.dwek@nasa.gov

[2]Department of Astronomy, University of Maryland, College Park MD 20742. e-mail: galliano@astro.umd.edu

and their metallicity (Madden et al. 2006). Low-metallicity galaxies exhibited very weak or no aromatic features. Observations of the 8-to-24 μm bands flux ratio obtained with the IRAC and MIPS instruments showed a correlation of this flux ratio with the galaxies' oxygen abundance (Engelbracht et al. 2005). Since the $\mathrm{IRAC}_{8\mu m}$ band is supposed to trace the strength of the aromatic features, and the $\mathrm{IRAC}_{24\mu m}$ that of the continuum emission from the hot non-aromatic dust component, this correlation seemed to confirm the trends discovered by *ISO*. A summary of these observations is given in Figure 1 (Galliano et al. 2008a).

Several interpretations have been given for this correlation: (1) Noting that the PAH-to-continuum intensity ratio correlates with the [NeIII]/[NeII] line ratio, which is a tracer of the young strongly ionizing stellar population, Madden et al. (2006) suggested that the paucity of PAH emission at low metallicity reflected their destruction by hard UV photons that are especially effective in destroying PAHs in dust-deficient environments; (2) O'Halloran et al. (2006) noted that the PAH-to-continuum intensity ratio correlates with the [FeII]/[NeII] line ratio as well. This line ratio is a tracer of interstellar shocks, suggesting that PAHs are more efficiently destroyed by shocks in low metallicity systems.

All previous explanations attribute the paucity of PAHs to destructive processes that are more efficient in the early stages of galaxy evolution. In contrast, Dwek (2005) suggested that the observed correlation reflects an evolutionary trend of the sources of interstellar PAHs with metallicity. PAHs and carbon dust are mostly produced in asymptotic giant branch (AGB) stars which, unlike massive stars, recycle their ejecta into the ISM after a significantly longer time of main sequence evolution. The observed correlation of PAH line intensities with metallicity is therefore a trend of PAH abundance with galactic age, reflecting the delayed injection of PAHs and carbon dust into the ISM by AGB stars in their final, post-AGB, phase of their evolution.

2. Phenomenological Modeling of the SEDs of Local Galaxies

Derivation of the PAH abundances in galaxies from their observed mid-IR spectral features is complicated by the nature of their emission mechanism. PAHs are stochastically-heated by the interstellar radiation field (ISRF) and consequently only a fraction of their population is copiously emitting IR radiation at any given time. Correcting for the mass of PAHs too cold to radiate at mid-IR wavelengths requires detailed modeling of their stochastic heating process, and therefore detailed knowledge of the ISRF. A self-consistent model must therefore be also able to reproduce the IR emission from the remaining dust population which is also stochastically-heated by the ISRF. The situation is further complicated by the

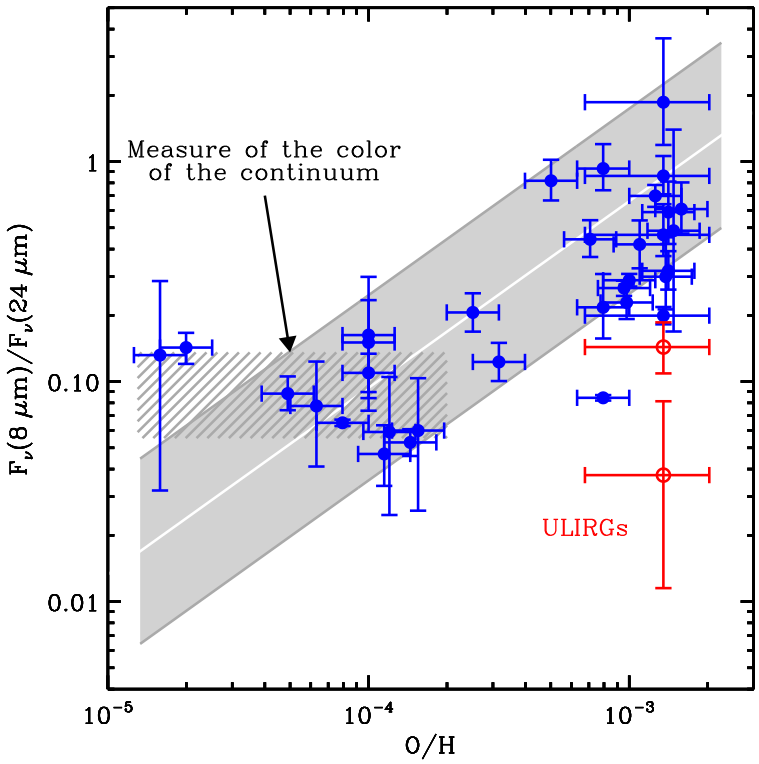

Fig. 1.— Mid-IR color as a function of the oxygen number abundance (after Galliano et al. 2008a). Our observed SEDs have been integrated over the $\mathrm{IRAC}_{8\,\mu m}$ and $\mathrm{MIPS}_{24\,\mu m}$ bandpasses, in order to produce this plot. The two open circles are the (U)LIRGs of our sample. The grey stripe is the $\pm 1\sigma$ linear correlation between log(O/H) and $\log\left(F_\nu(8\mu m)/F_\nu(24\mu m)\right)$. The hatched stripe shows the range of the ratio ($0.06 \lesssim F_\nu(8\mu m)/F_\nu(24\mu m) \lesssim 0.13$), which is a measure of the color of the silicate and graphite continuum, when the PAH features are weak. The figure illustrates the importance of knowing the mid-IR continuum emission in order to derive the intensity of the PAH bands.

fact that a significant fraction of the mid-IR emission originates from hot dust in H II regions radiating at the equilibrium dust temperature. Deriving the abundance of PAHs and other dust species in a galaxy requires therefore careful modeling of the stellar population that produces the ISRF that heats the dust in the diffuse ISM and the ionizing radiation that heats the dust in H II regions.

We constructed a self-consistent model for evolution of the stellar population and the composition of the ISM for the galaxies in our sample. The star formation history comprises of two distinct components: (1) a global continuous mode of star formation which is used to calculate the chemical evolution with a closed-box model, and the evolution of the stellar radiation using the PÉGASE stellar population code (Fioc & Rocca-Volmerange 1997); and

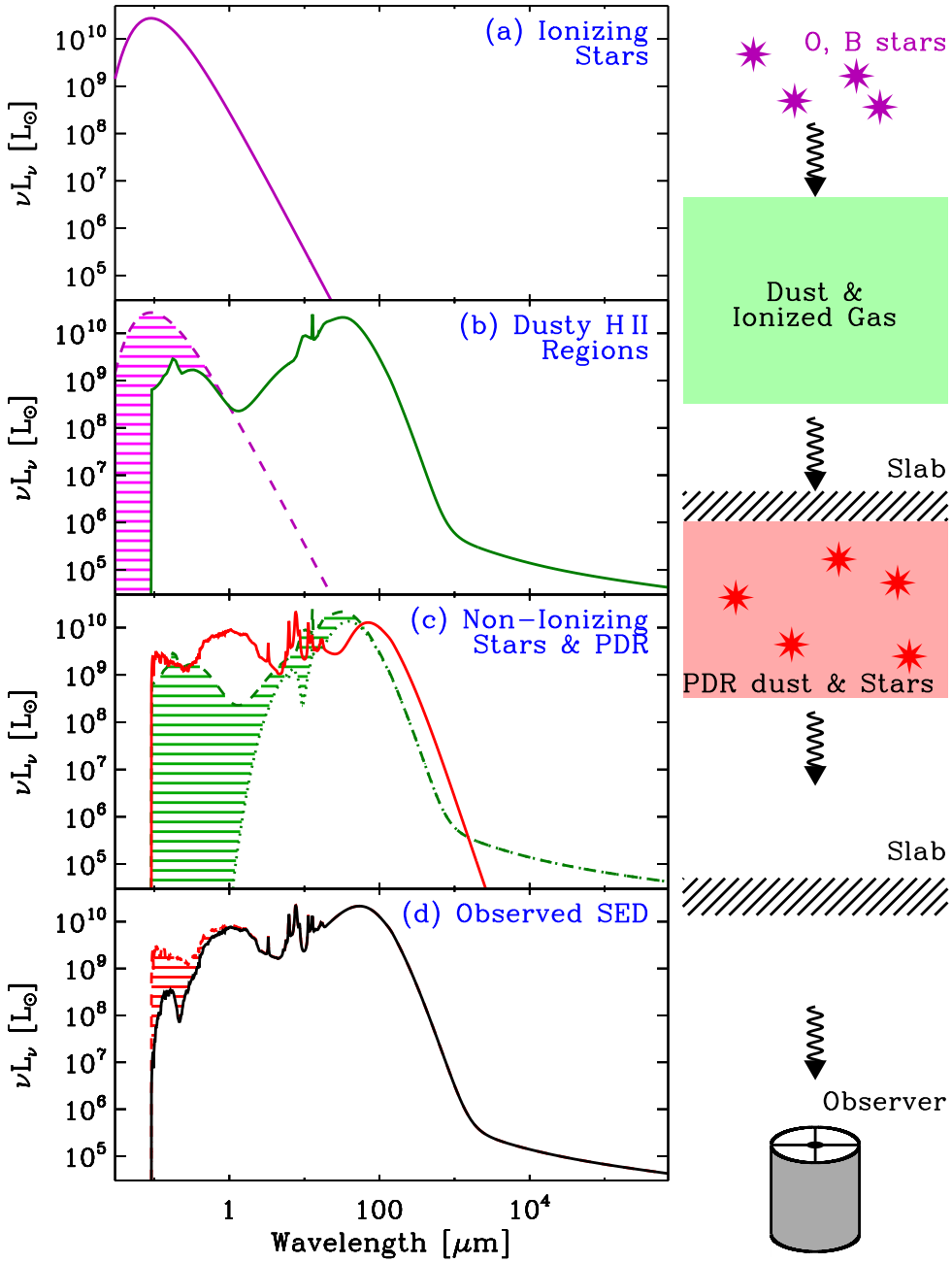

Fig. 2.— Schematic illustration of the of the model used to decompose the observed galactic SED into the various stellar and ISM emission components (Galliano et al. 2008a). **Panel (a)**: SED of the ionizing stars (purple curve). **Panel (b)**: IR spectrum of the dust in the H II regions (green curve). **Panel (c)**: Stellar emission and emission from dust residing in the neutral ISM (red curve). **Panel (d)**: The observed SED after passing through a slab of internal extinction (black curve). In each figure, the hatched region represents the emission from the previous panel that is absorbed by the relevant phase depicted in the panel.

(2) an "instantaneous burst" of star formation (age $\lesssim$ 10 Myr). This short-lived burst does not contribute significantly to the metallicity of the gas, and is tailored to fit the observed UV, optical, radio, and the IR emission from dust in H II regions. The continuous star formation component provides a self-consistent picture of the evolution of stellar colors and metallicity as a function of age in all the galaxies in the sample. The relative contribution of these two components, as well as the age of the galaxy are fully constrained by the UV-to-radio continuum emission. Details of the models are presented in Galliano et al. (2008a).

The following describes the steps used to decompose the observed galactic SEDs into the various stellar and ISM emission components. A schematic diagram of the modeling procedure is shown in Figure 2.

1. We first decompose the radio continuum into free-free and synchrotron emission in order to constrain the emission measure from the galaxy.

2. The resulting free-free continuum, together with observations of the mid-IR continuum between ~ 5 and ~ 60 μm are used to constrain the gas density and reradiated energy from the H II regions. We assume that any existing PAHs are destroyed inside the H II regions, and use a simple radiative transfer model (Galliano et al. 2008a) to calculate the absorbed radiation that is emitted as free-free emission from the gas, and thermal IR emission from the dust in the H II region.

3. Optical and near-IR broadband emission are used to constrain the radiation escaping from the H IIregions and that from the non-ionizing stars. They comprise the ISRF that heats the dust in PDRs.

4. The observed far-IR/submm SED constrains the dust emission from the PDRs. The PAH-to-dust mass fraction is constrained by the detailed fit of the features seen on the mid-IR spectrum.

5. Globally, the stellar luminosity absorbed by the gas and dust phases of the ISM is equal to the total reradiated and escaping power from the galaxy.

Figure 3 shows the fit of this model to the observed SED of the prototypical starburst galaxy M 82.

3. The Derived Trends of PAH and Dust Abundances with Metallicity

This model has been applied to the UV-to-radio observations of 35 nearby galaxies. The mid-IR spectra of these objects were observed by *ISO* or *Spitzer*, and are part of the samples

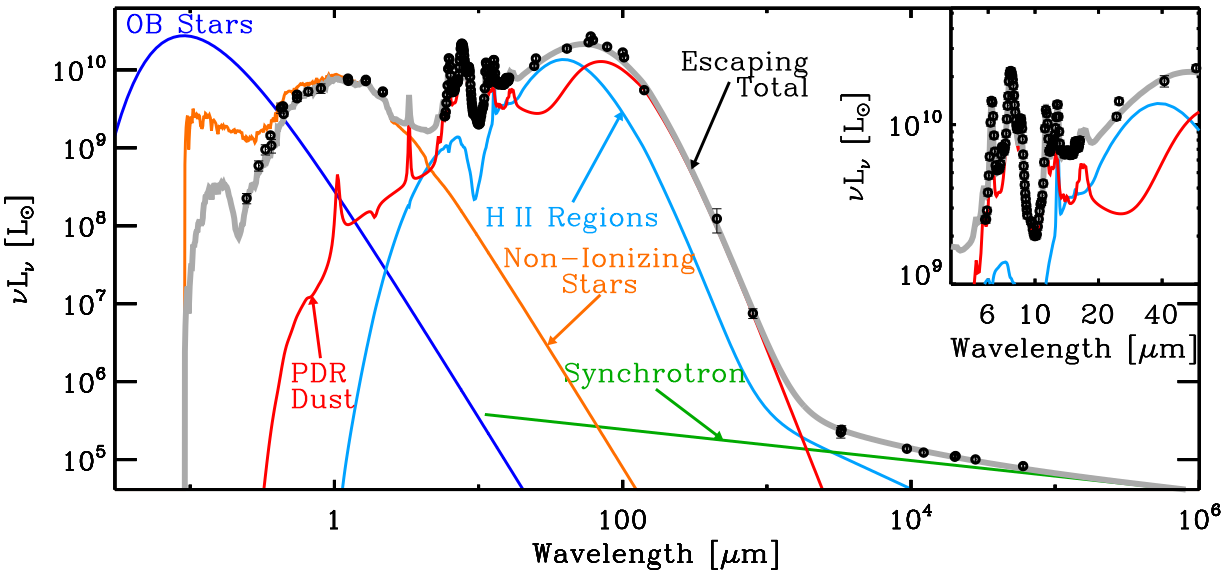

Fig. 3.— The observed SED of M 82 (filled circles) decomposed into the various emission components. **Dark blue curve**: intrinsic emission from OB stars; **Orange curve**: Intrinsic emission from non-ionizing stars. **Grey curve**: Model calculations of the escaping and reradiated stellar emission. **Light blue curve**: Contribution of the dust in H II region to the reradiated emission. **Red curve**: Contribution of the dust in H I region to the reradiated emission. **Red curve**: Synchrotron emission component.

presented by Madden et al. (2006) and Galliano et al. (2008b). Figure 4 shows the resulting PAH-to-gas and dust-to-gas mass ratios for each galaxy.

The left panel of figure 4 shows the trends of derived PAH-to-gas and dust-to-gas mass ratios as a function of the observed ISM metallicity of the galaxy. These results are consistent with the Galactic value derived by Zubko et al. (2004). The figure shows that both ratios increase sharply with metallicity, and that the PAH and dust follow two distinct evolutionary trends. The right panel of figure 4 highlights this differential evolution by showing the metallicity evolution of the PAH-to-dust mass ratio. This figure is the equivalent of figure 1, but with the mid-IR colors converted into PAH and dust abundances. These two figures are the relevant ones for interpreting the mid-IR colors versus metallicity trends in terms of a chemical evolution model.

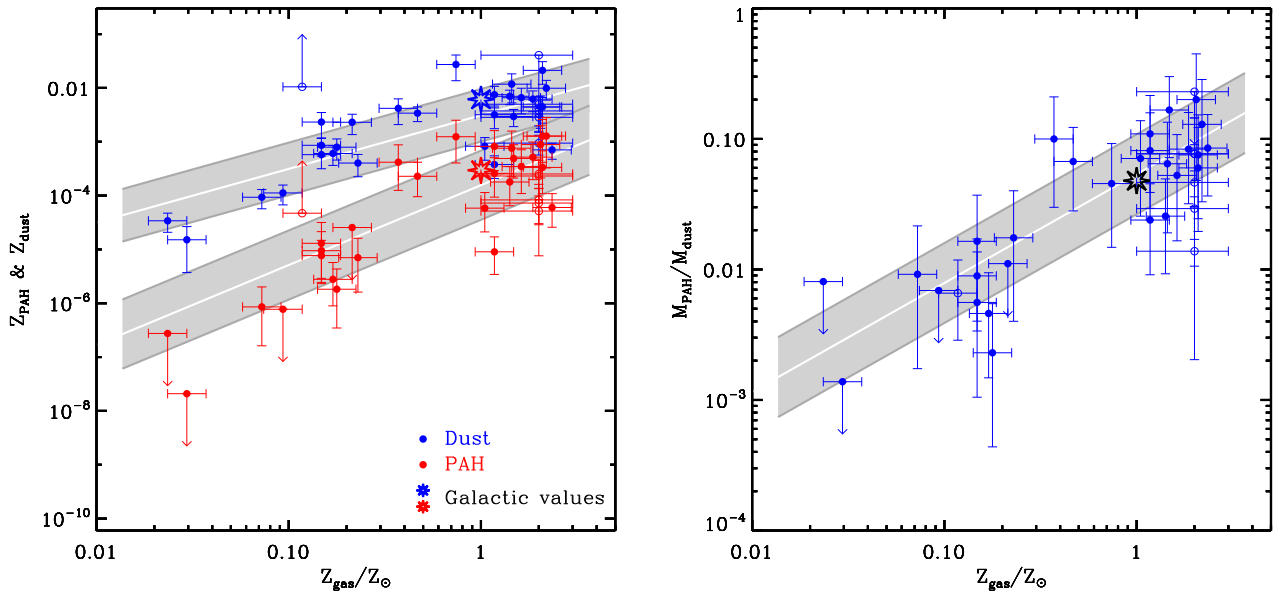

Fig. 4.— **Left panel**: Derived dust-to-gas mass ratios, $Z_{\rm PAH}$, for PAHs (red circles) and dust, $Z_{\rm dust}$, (blue circles) that give rise to the far-IR emission as a function of the gas metallicity. **Right panel**: Mass ratio of PAH-to-dust, as a function of metallicity. The circles correspond to galaxies and the open stars to the the diffuse Galactic ISM (Zubko et al. 2004). The filled circles are the reliable measurements, and the open circles are the ones which are considered uncertain. The grey stripes in both panels are the $\pm 1\sigma$ linear correlation, in logarithmic scale. These figures show the two distinct evolutionary trends of $Z_{\rm PAH}$ and $Z_{\rm dust}$ with metallicity.

4. The Delayed Injection of PAHs and Carbon Dust from AGB Stars

Infrared spectra of evolved Asymptotic Giant Branch (AGB) stars have revealed a large diversity of dust composition, recently reviewed by Waters (2004). The composition of the dust generally reflects the C/O ratio in their envelope. When this ratio is less than unity, the atmosphere reveals the presence of O-rich chemistry and the presence of several silicate dust species. When the C/O ratio exceeds unity, the outflow reveals the spectra of amorphous carbon, SiC, MgS, and in some cases PAHs as well. PAHs appear after the AGB phase, and are observed in C-rich planetary nebulae (Cohen & Barlow 2005), the evolutionary end phase of AGB stars. Some stars exhibit mixed chemistry, presumably because they were members of a binary system with opposite chemistry. Figure 5 depicts the C and O yield in AGB stars as a function of stellar mass, calculated by Karakas & Lattanzio (2003a,b). The mass yields were divided by the atomic weight so that the figures represent the relative number of C and O atoms returned to the ISM. We see that carbon dust will form in a narrow

range of stellar masses between 1.7 and 4.9 $M_\odot$. Figure 6 is an HR diagram depicting the Geneva Observatory evolutionary tracks of stars in the 0.8 to 40 $M_\odot$ mass range. The figure also shows the main-sequence (MS) lifetime of a select number of stars. The figure shows that the first C-rich stars will evolve off the MS only after $\sim$ 120 Myr, with most of the carbon dust injection occurring after $\sim$ 400 Myr. At this point, a galaxy would have been already enriched with metals produced by massive core-collapse supernovae which return their nucleosynthetic products "instantaneously" back to the ISM.

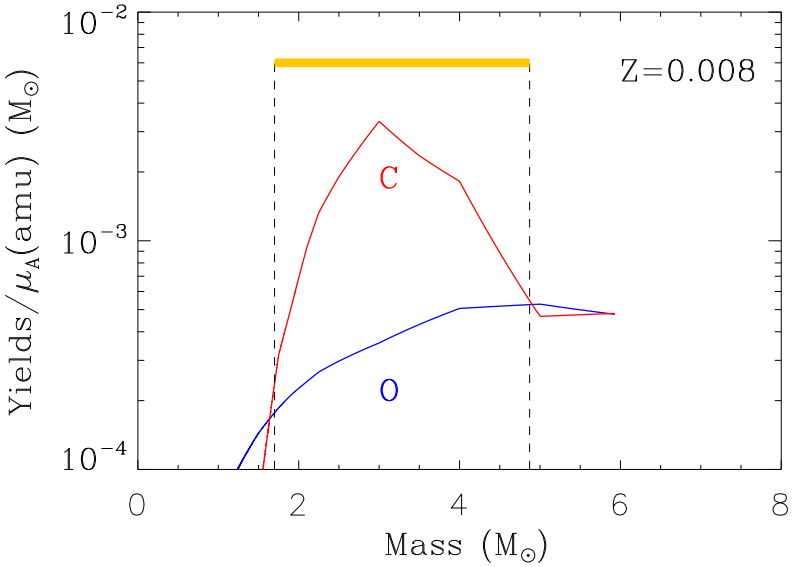

Fig. 5.— The carbon (red curve) and oxygen (blue curve) yields for different stellar masses with an initial metallicity of $Z = 0.008$. The yields are in solar masses, but divided by the atomic mass (in amu) of the different elements. Stars with masses between 1.7 and 4.9 $M_\odot$ have a C/O ratio larger then unity and will therefore form carbon dust. All other stars in the $\sim 1 - 8$ $M_\odot$ mass range will form silicate dust. Stellar yields were taken from Karakas & Lattanzio (2003a,b).

The delayed injection of PAHs by C-rich AGB stars into the ISM offers therefore the simplest and most straight-forward explanation for the observed paucity of PAHs in low-metallicity galaxies. To confirm the observed trend with metallicity we ran the chemical evolution model described in Dwek (1998) with parameters and yields described in Galliano et al. (2008a). The model follows the evolution of the elements in the gas and dust phases of the ISM, subject to formation in SNe and AGB stars, and destruction by SN blast waves in the ISM. Silicates and carbon dust (but not PAHs) can form in the ejecta of supernovae regardless of their global C/O ratio. In AGB stars, the formation of carbon or silicates is restricted to stars with the appropriate C/O ratio in their ejecta. The results of the model are shown in Figure 7. The figure clearly shows the separate evolutionary trends of SN- and AGB-condensed dust predicted by the models. The broad shaded area reflects the range of

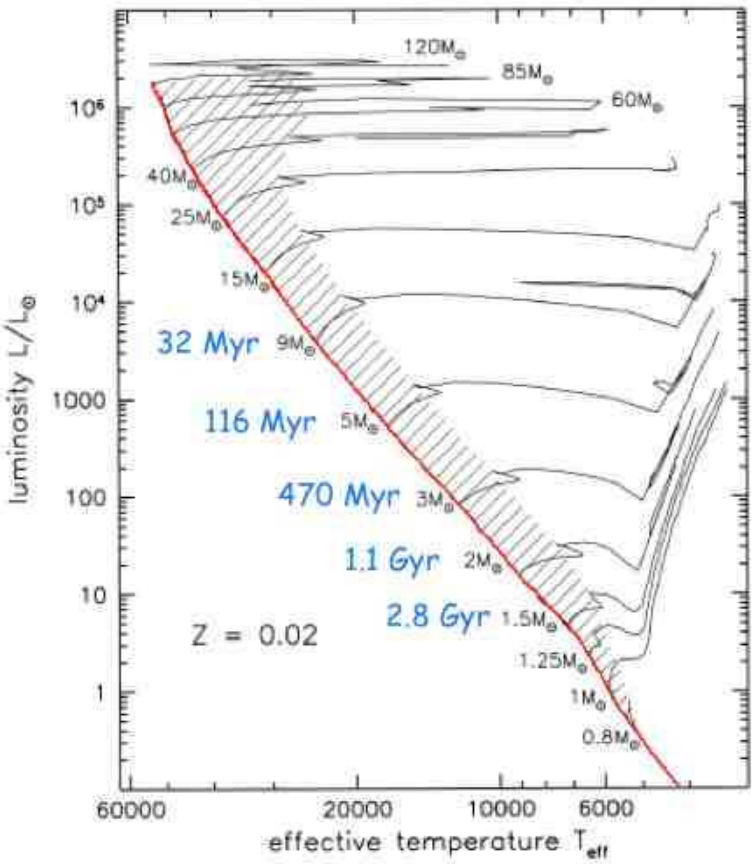

Fig. 6.— Geneva Observatory stellar evolutionary tracks as published in Sparke & Gallagher (2007). Curves are also labeled by the main-sequence lifetimes of the different stars.

possible evolutionary paths allowing for changes in the assumed star formation and grain destruction rates. The figure shows that the rise in PAH abundance with metallicity agrees very well with observations. At metallicities above $\sim Z_{\odot}$, corresponding to an age of about 3 Gyr, the model shows a decrease of PAH abundance with metallicity. At this epoch the last C-rich stars have evolved off the main sequence giving way to low mass ($M \lesssim 1.7$ M$_{\odot}$) O-rich stars that now inject silicate grains into the ISM. The figure also shows the good agreement between the predicted trend of SN-condensed dust with metallicity with that of the derived graphite and silicate dust.

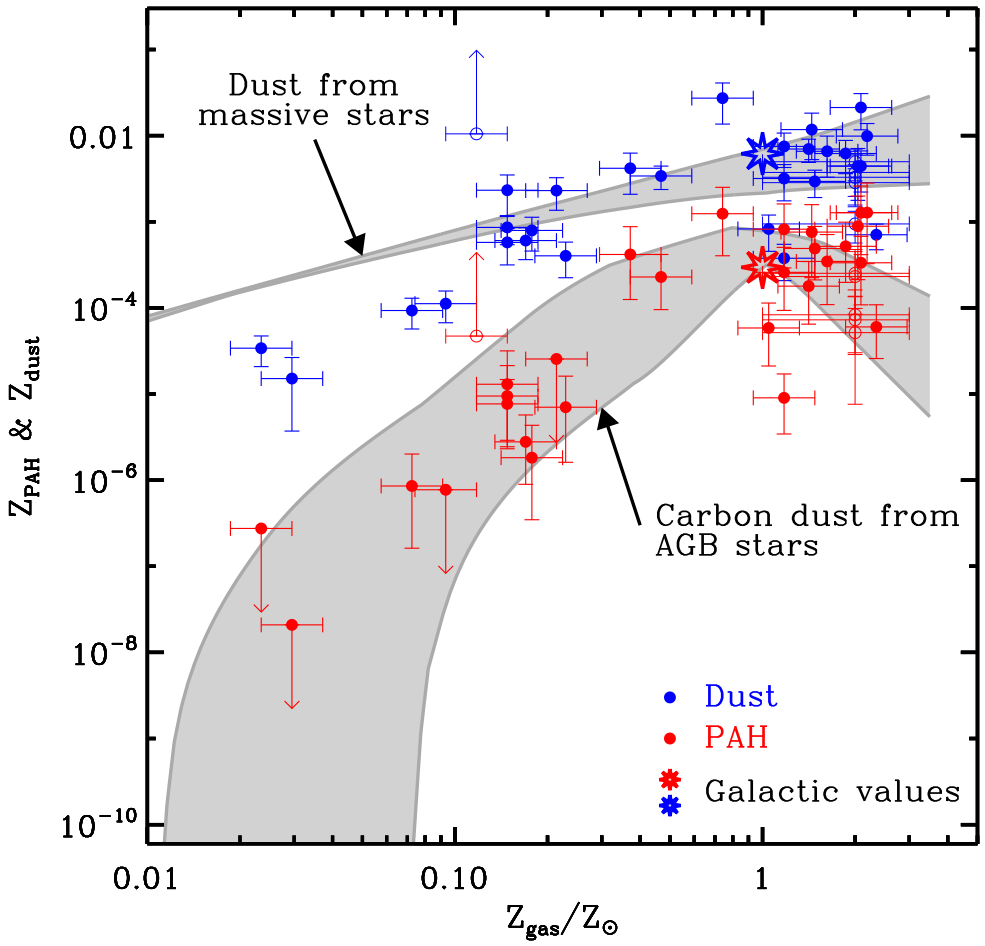

Fig. 7.— Comparison between the metallicity trends of the PAH abundance derived from the observed SED and those derived from the chemical evolution model. The figure highlights the different evolutionary trend of SN II- and AGB-condensed dust.

5. Summary

We constructed phenomenological models for the evolution of the stellar population and the metal and dust enrichment of the ISM, fully accounting for the observed panchromatic escaping and reprocessed emission from the stars and the ISM. The model for the evolution of dust includes the formation of the different dust species in the various sources, and their destruction by shocks in the ISM.

The results show that the observed paucity of PAHs in low metallicity galaxies is simply the result of the fact that C-rich AGB stars, the primary sources of PAHs, have not yet evolved off the main sequence. The alternative explanation that the paucity of PAHs in low metallicity galaxies reflects their more efficient destruction at the early stage of their evolution, is implicitly included in our model, since we assume that PAHs are completely destroyed by the ionizing radiation in H II regions. This destruction mechanism, as well as their destruction by shocks cannot explain the observed trend. Both explanations presume that PAHs are present at the early stages of galaxy evolution. Such explanation requires the efficient formation of PAHs, either in rare C-rich Wolf-Rayet stars, SN ejecta, or interstellar shocks, and the fine tuning of their destruction rate in order to explain the observed trend.

We conclude that the trend of PAH abundance versus metallicity is most naturally explained as the consequence of the delayed injection of PAHs into the ISM by relatively long-lived progenitors of the AGB stars in which they are formed. Our detailed chemical evolution models fully confirm this hypothesis.

This work is based on observations made with the *Spitzer Space Telescope*, which is operated by the Jet Propulsion Laboratory (JPL), California Institute of Technology under NASA contract 1407. Support for this work was provided by NASA and through JPL Contract 1255094.

REFERENCES

Cohen, M. & Barlow, M. J. 2005, MNRAS, 362, 1199

Dwek, E. 1998, ApJ, 501, 643

Dwek, E. 2005, in American Institute of Physics Conference Series, Vol. 761, The Spectral Energy Distributions of Gas-Rich Galaxies: Confronting Models with Data, ed. C. C. Popescu & R. J. Tuffs, 103–+

Engelbracht, C. W., Gordon, K. D., Rieke, G. H., et al. 2005, ApJ, 628, L29

Fioc, M. & Rocca-Volmerange, B. 1997, A&A, 326, 950

Galliano, F., Dwek, E., & Chanial, P. 2008a, ApJ, 672, 214

Galliano, F., Madden, S. C., Tielens, A. G. G. M., Peeters, E., & Jones, A. P. 2008b, ArXiv e-prints, 801

Karakas, A. I. & Lattanzio, J. C. 2003a, Publications of the Astronomical Society of Australia, 20, 393

Karakas, A. I. & Lattanzio, J. C. 2003b, Publications of the Astronomical Society of Australia, 20, 279

Madden, S. C., Galliano, F., Jones, A. P., & Sauvage, M. 2006, A&A, 446, 877

O'Halloran, B., Satyapal, S., & Dudik, R. P. 2006, ApJ, 641, 795

Sparke, L. S. & Gallagher, III, J. S. 2007, Galaxies in the Universe: An Introduction (Galaxies in the Universe: An Introduction. Second Edition. By Linda S. Sparke and John S. Gallagher, III. ISBN-13 978-0-521-85593-8 (HB); ISBN-13 978-0-521-67186-6 (PB). Published by Cambridge University Press, Cambridge, UK, 2007.)

Waters, L. B. F. M. 2004, in Astronomical Society of the Pacific Conference Series, Vol. 309, Astrophysics of Dust, ed. A. N. Witt, G. C. Clayton, & B. T. Draine, 229–+

Zubko, V., Dwek, E., & Arendt, R. G. 2004, ApJS, 152, 211